

Figure 7. Activation energy of the ac (1 V) ionic conductivity in $\text{PMEO}_n\text{-LiX}$ systems.

conductor. The dc ionic conductivity of thus polarized hybrid films can be recovered temporarily by a prolonged ac potential supply.

Activation Energy for Ionic Conduction in $\text{PMEO}_n\text{-LiX}$ Systems. The temperature dependence of the ionic conductivity of $\text{PMEO}_n\text{-LiX}$ systems is shown in the linear Arrhenius-type plots, $\log \sigma_i$ vs. T^{-1} , in Figure 6. Generally, in polymer/MX hybrid solid-state ionic conductors, such plots show curved lines due to the contribution of the first term in parentheses in eq 2 (due to

the existence of T_g). However, when T_g is far lower than the temperature employed for the conductivity measurement, the first term in the parentheses becomes negligibly small. In such cases, eq 2 can be simplified to

$$\sigma_i = \sigma_0 \exp \left[-\frac{E + W/2\epsilon}{kT} \right] \quad (3)$$

so that linear Arrhenius plots are obtained.

From Figure 7 it is noticed that (i) the activation energy for ionic conduction, E_a increases with an increase of LiX content, (ii) the increasing feature of E_a is more outstanding in the $\text{PMEO}_n\text{-LiClO}_4$ systems than that in the $\text{PMEO}_n\text{-LiPF}_6$ systems, (iii) the E_a of the $\text{PMEO}_n\text{-LiClO}_4$ systems is much larger than that in the $\text{PMEO}_n\text{-LiPF}_6$ systems, and (iv) there is a relatively small difference in E_a among $\text{PMEO}_n\text{-LiClO}_4$ systems with different n if the same lithium salt is used. (i) is related to the increase of microviscosity with increasing the salt content. (ii) and (iii) reflect the fact that the increment in microviscosity on adding LiX is more drastic in the $\text{PMEO}_n\text{-LiClO}_4$ systems and that the solubility of LiClO_4 is worse than that of LiPF_6 . (iv) suggests that the ionic conductivity of $\text{PMEO}_n\text{-LiX}$ systems is mostly influenced by the preexponential term of eq 3, as the large difference in the ionic conductivity (especially see the ionic conductivity at low $[\text{LiClO}_4]$ in Figure 3) is not reflected in the E_a value.

Acknowledgment. This work is partially supported by a Grant-in-Aid for Scientific Researches from the Ministry of Education, Science and Culture, Japan.

Registry No. LiClO_4 , 7791-03-9; LiPF_6 , 21324-40-3; poly(oxyethylene)monomethyl ether methacrylate polymer, 87105-87-1; poly(oxyethylene)acetate, 27613-77-0.

Formation of a Polymer-Supported Catalyst from Anchored RhO_3 Clusters: Aggregation with Segregation of the Metals

J. Lieto,[†] M. Wolf,^{††} B. A. Matrana,[†] M. Prochazka,[†] B. Tesche,[‡] H. Knözinger,[‡] and B. C. Gates^{*†}

Center for Catalytic Science and Technology, Department of Chemical Engineering, University of Delaware, Newark, Delaware 19716, and Physikalisch-Chemisches Institut der Universität, 8000 München 2, West Germany, and Fritz-Haber-Institut der Max-Planck-Gesellschaft, 1000 Berlin 338 FRG (Received: August 24, 1984)

Supported molecular metal clusters were prepared by the ligand association reaction involving the phosphine groups of poly(styrene-co-divinylbenzene-co-p-styryldiphenylphosphine) and $[\text{H}_2\text{RhOs}_3(\text{acac})(\text{CO})_{10}]$ to give $[\text{H}_2\text{RhOs}_3(\text{acac})(\text{CO})_{10}\text{Ph}_2\text{P}-\text{P}]$. This molecular analogue was used as a precursor of a supported metal catalyst, its activity being probed with the isomerizations of but-1-ene and the hydrogenation of ethylene, and its structure being characterized by infrared spectroscopy, X-ray photoelectron spectroscopy, and transmission electron microscopy. The results show that the initial bimetallic cluster broke up with segregation of the metals. The infrared spectra show that the cluster breakup gave stable triosmium carbonyl clusters, which account for the isomerization activity. The activity for hydrogenation is attributed to Rh metal; the electron microscopy suggested the presence of metal particles <1.0 nm in diameter.

Introduction

Supported bimetallic catalysts are finding an increasing number of technological applications, including re-forming of light petroleum fractions.¹ Since the metal species on the support are typically aggregates or crystallites with diameters of only 1–10 nm, which are nonuniform in size, shape, and catalytic activity, it is difficult to obtain precise structural characterizations and to measure relations between structure and catalytic performance.

Our objective was to investigate a supported bimetallic catalyst initially having a simple structure—analogue to that of a molecular metal cluster. The evolution of the structure was followed with both spectroscopic and catalytic reaction probes. The support was chosen to be poly(styrene-co-divinylbenzene), since this polymer is nearly inert and allows straightforward synthesis of bound organometallics;² the metal cluster precursor was chosen

[†] University of Delaware.

^{††} Physikalisch-Chemisches Institut der Universität.

[‡] Fritz-Haber-Institut der Max-Planck-Gesellschaft.

(1) Sinfelt, J. H. *Bimetallic Catalysts—Discoveries, Concepts, and Applications*; Wiley: New York, 1983.

(2) Lieto, J.; Milstein, D.; Albright, R. L.; Minkiewicz, J. V.; Gates, B. C. *CHEMTECH* 1983, 13, 46.

TABLE I: Infrared Characterization of Molecular Clusters and Their Supported Analogues

sample	solvent or phase	ν_{CO} , cm^{-1}	ref
$[\text{H}_2\text{RhOs}_3(\text{acac})(\text{CO})_{10}]$	cyclohexane	2073 s, 2065 msh, 2037 vs, 2015 s, 1999 msh, 1985 msh, 1973 m	7
$[\text{H}_2\text{RhOs}_3(\text{acac})(\text{CO})_{10}\text{PPh}_3]$	cyclohexane	2085 m, 2061 s, 2034 s, 1997 s, 1989 ssh, 1981 w, 1969 m, 1961 w	7
$[\text{H}_2\text{RhOs}_3(\text{acac})(\text{CO})_{10}\text{PPh}_2-\text{O}]$	membrane	2085 m, 2061 s, 2034 s, 1997 s, 1978 sh, 1966 m	this work ^a
$[\text{H}_2\text{Os}_3(\text{CO})_{10}\text{PPh}_3]$	CH_2Cl_2	2105 m, 2066 s, 2051 s, 2025 vs, 2017 vs, 2004 m, 1983 m, 1971 m	this work ^b
$[\text{H}_2\text{Os}_3(\text{CO})_9\text{PPh}_3]$	CH_2Cl_2	2093 m, 2053 s, 2015 ssh, 2012 vs, 2004 vs, 1991 m, 1976 m, 1962 w	this work
$[\text{H}_2\text{Os}_3(\text{CO})_9(\text{alkene})\text{PPh}_2-\text{O}]$	membrane	2089 m, 2045 s, 2010 vs	5, 6

^a A closely similar spectrum was reported by Farrugia et al.⁷ ^b A similar spectrum was reported by Deeming and Hasso.⁸

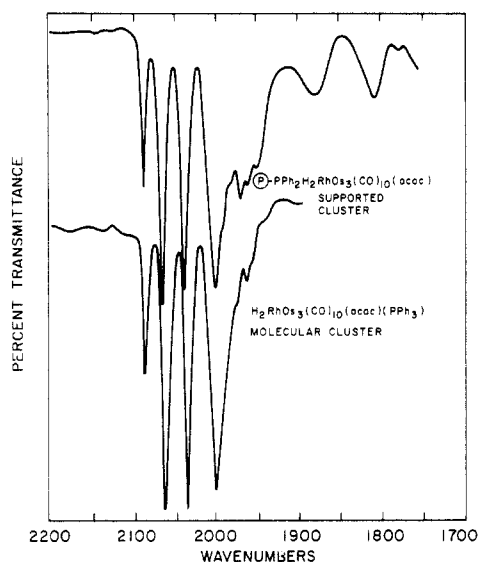


Figure 1. Infrared spectra of $[\text{H}_2\text{RhOs}_3(\text{CO})_{10}(\text{acac})\text{PPh}_3]$ and its polymer-supported analogue. The broad bands at 1800 and 1875 cm^{-1} are indicative of the polymer backbone.

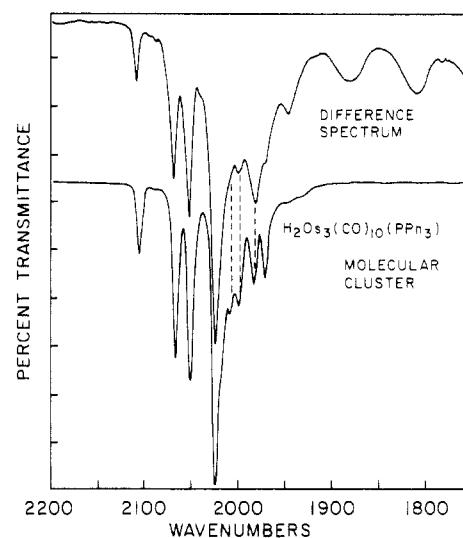


Figure 2. Infrared spectra of sample 1 initially in the form of $[\text{H}_2\text{RhOs}_3(\text{acac})(\text{CO})_{10}\text{Ph}_2\text{P}-\text{O}]$ after a 30-min treatment in CO at 60 $^{\circ}\text{C}$; the spectrum of the initial cluster was subtracted to give the spectrum shown, which is similar to that of $[\text{H}_2\text{Os}_3(\text{CO})_{10}\text{PPh}_3]$.

to be $[\text{H}_2\text{RhOs}_3(\text{acac})(\text{CO})_{10}]$, since there is literature concerning both $\text{Rh}^{3,4}$ and $\text{Os}^{3,5}$ catalysts in various forms on the polymeric support. The catalytic probe reactions were isomerization and hydrogenation of alkenes, which occur at temperatures sufficiently low for stability of the catalyst support and with rates that are sensitive to the catalyst structure. The results show that RhOs_3 clusters were initially anchored intact to the support through phosphine ligands and that the clusters broke up to give catalytically active species: the metals became segregated, with the Rh aggregating into crystallites and the Os remaining in the form of anchored trinuclear clusters.

Results and Discussion

Preparation of the Supported RhOs_3 Cluster. The supported metal cluster was synthesized by the reaction of $[\text{H}_2\text{RhOs}_3(\text{acac})(\text{CO})_{10}]$ with membranes of the block copolymer poly(styrene-*co*-divinylbenzene-*co-p*-styryldiphenylphosphine). The supported organometallic species was characterized by comparison of its infrared spectrum in the carbonyl region with those of known molecular clusters and complexes. The infrared data, summarized in Table I and Figure 1, demonstrate the presence of the 62-electron polymer-supported cluster $[\text{H}_2\text{RhOs}_3(\text{acac})(\text{CO})_{10}\text{Ph}_2\text{P}-\text{O}]$ (the analogue of $[\text{H}_2\text{RhOs}_3(\text{acac})(\text{CO})_{10}\text{PPh}_3]$; there is no evidence in the spectrum of any other metal carbonyl). We infer that the synthesis reaction was the simple ligand association of the coordinatively unsaturated 60-electron cluster $[\text{H}_2\text{RhOs}_3(\text{acac})(\text{CO})_{10}]$ with the $-\text{PPh}_2$ groups of the polymer, which was expected from the analogous solution chemistry.⁷ The

elemental analysis (Table II) is consistent with this inference; it shows that only about 9% of the $-\text{PPh}_2$ groups in the polymer were coordinated to clusters. The analogy with the molecular cluster $[\text{H}_2\text{RhOs}_3(\text{acac})(\text{CO})_{10}\text{PPh}_3]$ implies that the phosphine ligand is bonded to the Rh atom.⁷

Breakup of the Supported RhOs_3 Cluster during Reaction with CO. To allow characterization of the reactivity of the supported bimetallic cluster, sample 1, incorporating the original bound cluster $[\text{H}_2\text{RhOs}_3(\text{acac})(\text{CO})_{10}\text{Ph}_2\text{P}-\text{O}]$, was placed in a controlled-atmosphere infrared cell in a flow system. CO at 1 atm flowed over the membrane for 30 min at 60 $^{\circ}\text{C}$ and was replaced by He for 30 min to purge all traces of CO gas; the infrared spectrum of the membrane was then recorded. Bands indicative of the original anchored cluster were observed with reduced intensities, and a new set of bands was evident (2066, 2051, 2025, 2017 cm^{-1}). To determine a spectrum characteristic of the new species in the mixture, the spectrum of the original cluster was subtracted computationally. The spectrum resulting from this subtraction (Figure 2) is indicative of the cluster $[\text{H}_2\text{Os}_3(\text{CO})_{10}\text{PPh}_2-\text{O}]$, as shown by a comparison with the spectrum of the molecular analogue $[\text{H}_2\text{Os}_3(\text{CO})_{10}(\text{PPh}_3)]$ (Figure 2, Table I). We infer, therefore, that the supported 62-electron cluster $[\text{H}_2\text{RhOs}_3(\text{acac})(\text{CO})_{10}\text{Ph}_2\text{P}-\text{O}]$ reacted with CO, leading to breakup of the cluster with retention of the trinuclear framework. Similarly, the 60-electron cluster $[\text{H}_2\text{RhOs}_3(\text{acac})(\text{CO})_{10}]$ reacts instantly with CO in solution to produce $[\text{Rh}(\text{acac})(\text{CO})_2]$ and $[\text{HOs}_3(\text{CO})_{11}]$.⁷

Catalytic Hydrogenation of Ethylene. The polymer-supported cluster $[\text{H}_2\text{RhOs}_3(\text{acac})(\text{CO})_{10}\text{Ph}_2\text{P}-\text{O}]$ was tested as a catalyst for ethylene hydrogenation at temperatures of 25 to 110 $^{\circ}\text{C}$ with partial pressures of H_2 and ethylene equal to 0.81 and 0.21 atm,

(3) For a review of polymer-supported metal-complex catalysts, see: Pittman, C. U. In "Comprehensive Organometallic Chemistry"; Wilkinson, G., Stone, F. G. A., Abel, E. W., Eds.; Pergamon Press: Oxford, 1982; Vol. 8, p 553.

(4) Jarrell, M. S.; Gates, B. C.; Nicholson, E. D. *J. Am. Chem. Soc.* **1978**, *100*, 5727.

(5) Freeman, M. B.; Patrick, M. A.; Gates, B. C. *J. Catal.* **1982**, *73*, 82.

(6) N'Guini-Effa, J. B.; Lieto, J.; Aune, J. P. *J. Mol. Catal.* **1982**, *15*, 367.

(7) Farrugia, L. J.; Howard, J. A. K.; Mitrprachachon, P.; Stone, F. G. A.; Woodward, P. *J. Chem. Soc., Dalton Trans.* **1981**, 171.

(8) Deeming, A. J.; Hasso, S. *J. Organomet. Chem.* **1976**, *114*, 313.

TABLE II: Analysis of Polymers [H₂RhOs₃(acac)(CO)₁₀Ph₂P-⊙]

sample no.	composition of support ^a		elemental anal., wt %			molar ratio	
	crosslinking, % divinylbenzene	% p-styryldiphenyl- phosphine	P	Rh	Os	P/Rh	Os/Rh
1	2	5	2.15	0.62	3.3	11.5	2.9
2	5	10		1.79	9.8		2.9

^aDetermined by composition of monomer mixture used in the synthesis.

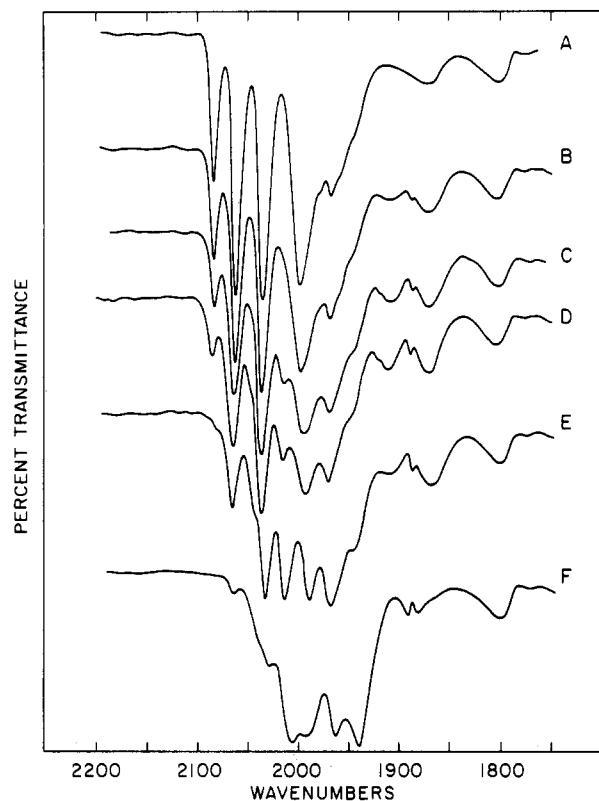


Figure 3. Changes in the carbonyl spectrum of sample 1 during its use as a catalyst for ethylene hydrogenation ($P_{H_2} = 0.81$ atm and $P_{C_2H_4} = 0.21$ atm): (A) sample 1 freshly prepared under helium at 27 °C; (B) after exposure to flowing C₂H₄ and H₂ for 100 min at 40 °C; (C) after exposure to flowing C₂H₄ and H₂ for 20 min at 85 °C; (D) after exposure to flowing C₂H₄ and H₂ for 10 min and 104 °C; (E) after exposure to flowing C₂H₄ and H₂ for 30 min at 104 °C; (F) after exposure to flowing C₂H₄ and H₂ for 6 h at 110 °C. The resulting solid was brown and had a carbonyl spectrum closely resembling that of [H₂Os₃(CO)₉(alkene)-PPh₃]. Carbonylation of the sample at 100 °C for 1 h did not change the spectrum.

respectively. The catalyst membrane (sample 1) was mounted in an infrared cell, which was also a flow reactor designed to allow simultaneous recording of the infrared spectrum of the functioning catalyst and (by on-line gas chromatography) the conversion of the reactants.

Neither conversion of reactant nor a change in the infrared spectrum was observed at room temperature during the first hour on stream, confirming the lack of activity of the coordinatively saturated cluster. A conversion of 0.02% was measured after 1.5 h on stream; this increased to 0.04% after 4 h. There were no detectable changes in the spectrum. The temperature was then increased to 40 °C over a 10-min period, and the catalytic activity was observed to increase with time on stream at this temperature as catalytically active species evidently formed. The conversion changed from 0.05 to 0.12% over a 100-min period, and simultaneously the bands in the carbonyl region decreased in intensity, the relative intensities remaining unchanged; no new bands were observed (Figure 3).

The sample was then heated at 0.5 °C/min in the flowing reactants. When the temperature reached 85 °C, new bands appeared at 2046 and 2013 cm⁻¹; the intensities of the bands

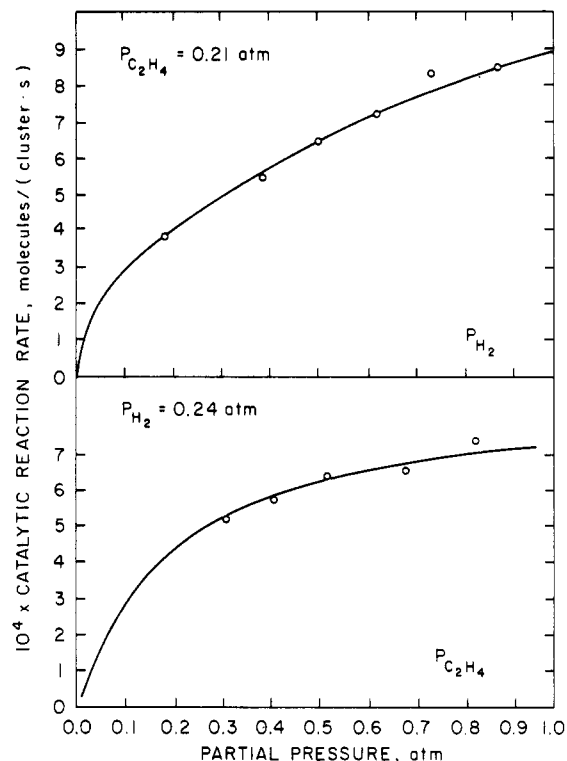


Figure 4. Kinetics of ethylene hydrogenation at 43 °C catalyzed by a polymer (sample I) characterized by spectrum F, Figure 3. The curves represent the fit of eq 1 with the parameter values stated in the text.

characteristic of the original cluster had decreased further; and the 2085-cm⁻¹ band had shifted to 2083 cm⁻¹, while that at 1997 cm⁻¹ had broadened (Figure 3). At 104 °C, the 2083-cm⁻¹ band had almost disappeared, and there were intense bands at 2046, 2013, 1989, and 1967 cm⁻¹. The changes became increasingly pronounced as the experiment continued (Figure 3). When the temperature reached 110 °C, it was held constant for 6 h, after which the sample had turned brown and had developed an infrared spectrum closely resembling that of [H₂Os₃(alkene)(CO)₉Ph₂P-⊙] (Figure 3, Table I). Exposure to flowing CO at 1 atm and 100 °C for 1 h did not change this spectrum. These results indicate that the bimetallic clusters had broken up with retention of the stable Os-Os bonds—and presumably with formation of mononuclear Rh complexes.

During these and similar experiments, the catalytic activity of the sample for alkene hydrogenation passed through a maximum: This result suggests that the rhodium had been aggregated to give catalytically active metal, which lost activity with changes in the average coordination number of Rh upon further aggregation. Formation of small Rh aggregates from hexarhodium clusters in the presence of hydrogen has been observed before in poly(styrene-co-divinylbenzene) membranes.⁴

A steady-state catalytic activity was easily attained at 43 °C with the sample which had been held at 110 °C for 6 h. At this condition, the conversions were less than 1%; they were shown experimentally to be differential, determining reaction rates directly. Therefore, the feed composition was varied systematically to allow a determination of reaction kinetics. The reaction rate data (Figure 4) were fitted to several simple rate equations of the Langmuir form with standard nonlinear least-squares regression

techniques. The equation that best represented the data is the following:

$$r = \frac{kK_{C_2H_4}P_{C_2H_4}K_{H_2}^{1/2}P_{H_2}^{1/2}}{1 + K_{C_2H_4}P_{C_2H_4}} \quad (1)$$

where r is the rate in molecules/(cluster-s); P the partial pressure (varied between 0.1 and 0.9 atm); k the rate constant; and $K_{C_2H_4}$, according to the Langmuir formalism, the ethylene equilibrium adsorption constant, equal to 5.5 ± 0.5 atm. The product $kK_{C_2H_4}K_{H_2}^{1/2}$ is equal to $(9.5 \pm 1.0) \times 10^{-3}$ molecules/(cluster-s·atm^{3/2}). The good fit of the data to this empirical rate equation is shown in Figure 4.

This form of kinetics is similar to that observed for ethylene hydrogenation catalyzed by rhodium particles on poly(styrene-co-divinylbenzene) and other supports.⁴

Catalytic Isomerization of But-1-ene. In a separate set of experiments, a polymer membrane incorporating the bimetallic cluster (sample 2) was used as a catalyst for conversion of but-1-ene, in the presence of hydrogen (to test for hydrogenation activity) and in the absence of hydrogen (to test for isomerization activity). The alkene isomerization reaction is catalyzed by polymer-supported triosmium clusters.^{5,6} The triosmium clusters, on the other hand, have only little activity for alkene hydrogenation in comparison with isomerization.⁵

A sample of catalyst was again held in the flow reactor allowing simultaneous measurement of the conversion and the infrared spectrum of the functioning catalyst. When but-1-ene and hydrogen at partial pressures of 0.41 and 0.66 atm, respectively, were allowed to flow over the catalyst at 27 °C, no conversion was observed. Under these conditions, the infrared spectrum of the membrane was indistinguishable from that of the original coordinatively saturated $[H_2RhOs_3(acac)(CO)_{10}Ph_2P-\text{D}]$.

When the temperature was raised to 50 °C with the reactant partial pressures unchanged, catalytic hydrogenation was observed (the conversion increased from 0.44 to 0.54% over a 70-min period), but no isomerization products were detected. A small decrease in the intensities of the bands in the carbonyl region was observed, with no discernible change in the relative intensities. H_2 was then replaced by He in the feed stream, and the temperature was raised to 74 °C; a conversion of 0.05% of but-1-ene into *trans*-but-2-ene was then observed. Replacement of He by H_2 led to the simultaneous occurrence of catalytic isomerization (conversion = 0.055%) and hydrogenation (conversion = 1.38%). Presuming that the conversions were differential, we calculate that the hydrogenation rate was 25 times greater than the isomerization rate. Evidently, species with catalytic activity for isomerization as well as hydrogenation had been formed from the bimetallic cluster.

Steady-state conversion was not attained with a constant feed flow rate and composition at this temperature; the hydrogenation rate had become 25% lower after a 10-h on-stream period, whereas the isomerization rate had become 10% higher after the same period. Changes in the infrared spectrum became evident after 2 h on stream.

These changes in the spectrum were similar to those observed with sample 1 when it was brought in contact with ethylene and H_2 . New band appeared at 2013 and 2046 cm^{-1} , as shown in Figure 5, indicative of the formation of $H_2Os_3(alkene)-(CO)_9Ph_2P-\text{D}$ (Table I), which is therefore suggested to be the catalytically active species for alkene isomerization.^{5,6} The catalyst was then heated to 112 °C and held at this temperature for 4 h with the partial pressures of H_2 and but-1-ene being 0.66 and 0.41 atm, respectively. The observed hydrogenation rate was then 2.8 times greater than the isomerization rate. Infrared spectra of the catalyst were recorded during this period and showed that the triosmium cluster had formed in increasing amounts. Figure 5 shows that the initial strong band at 2083 cm^{-1} had almost disappeared while new bands appeared at 2046, 2013, 1989, and 1967 cm^{-1} .

After this 4-h period, hydrogen was replaced by helium, and the temperature was held at 110 °C. Under these conditions, a

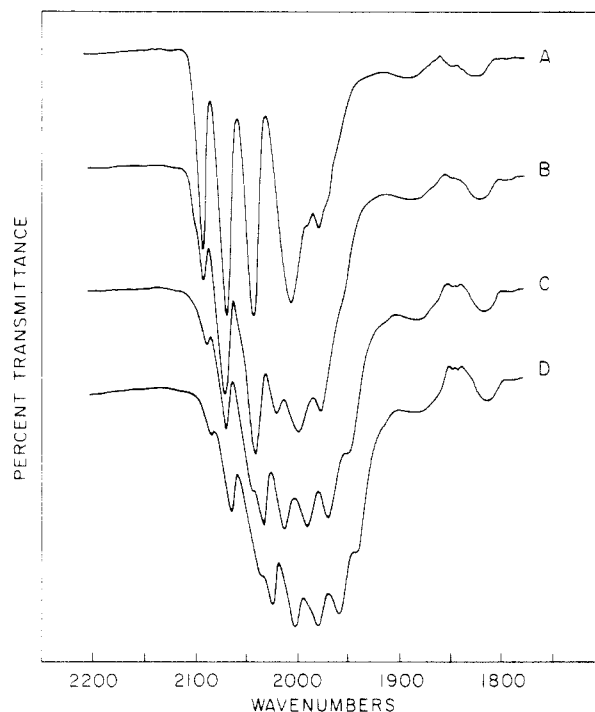


Figure 5. Changes in the carbonyl spectrum of sample 2 during its use as a catalyst for but-1-ene isomerization [$P_{C_4} = 0.41$ and P_{H_2} (or $P_{He}) = 0.66$ atm]: (A) sample 2 freshly prepared under helium at 27 °C; (B) after exposure to flowing but-1-ene and H_2 for 2 h at 70 °C; (C) after exposure to flowing but-1-ene and H_2 for 4 h at 112 °C; (D) after exposure to flowing but-1-ene and He for 6 h at 110 °C.

steady state was achieved for the isomerization reaction. Conversions were less than 2% and were shown experimentally to be differential. With helium used as a diluent, the partial pressure of but-1-ene was varied from 0.1 to 0.9 atm. Kinetics data were obtained and fitted to several simple equations of the Langmuir form with standard regression techniques. The data are best represented by the following equation:

$$r = \frac{kK_{C_4H_8}P_{C_4H_8}}{1 + K_{C_4H_8}P_{C_4H_8}} \quad (2)$$

where r is the rate in molecules/(cluster-s); $P_{C_4H_8}$ the but-1-ene partial pressure; k the rate constant, equal to $(2.56 \pm 0.3) \times 10^{-3}$ molecules/(cluster-s); and K the but-1-ene equilibrium adsorption constant, equal to 0.96 ± 0.1 atm⁻¹. The fit of the data provided by this equation is shown in Figure 6.

Characterization of Used Catalysts by Electron Microscopy. Since particles of rhodium metal seemed to be likely candidates as the hydrogenation catalysts, an electron microscope was used to search for metal particles in the used catalysts. The electron micrographs (Figure 7) show cross sections through two polymer membranes which had been used in catalytic reaction experiments. The micrographs of Figure 7 provide evidence of the metals. The micrographs of Figure 7, a and c, also demonstrate that the metals were nonuniformly distributed through the membrane (presumably because of a mass transport restriction in the cluster attachment process). Zones with high metal contents extending from the surfaces of the membranes are evident, their thicknesses being about 1.0 μm . The densities of metal in these zones are different in the two membranes.

We expect that the triosmium clusters (about 0.6 nm in diameter) would be too small to resolve with the microscope; we might therefore suggest that the high-magnification micrographs of Figure 7, b and d, provide evidence of Rh aggregates. However, the micrographs cannot be interpreted unequivocally since they were produced by the superposition of phase and amplitude contrast in relatively thick specimens. There is no doubt that metal aggregates with diameters >1 nm were not present in the membranes. High-resolution dark-field microscopy did not improve the resolution; there were unfavorable signal-to-noise ratios, since

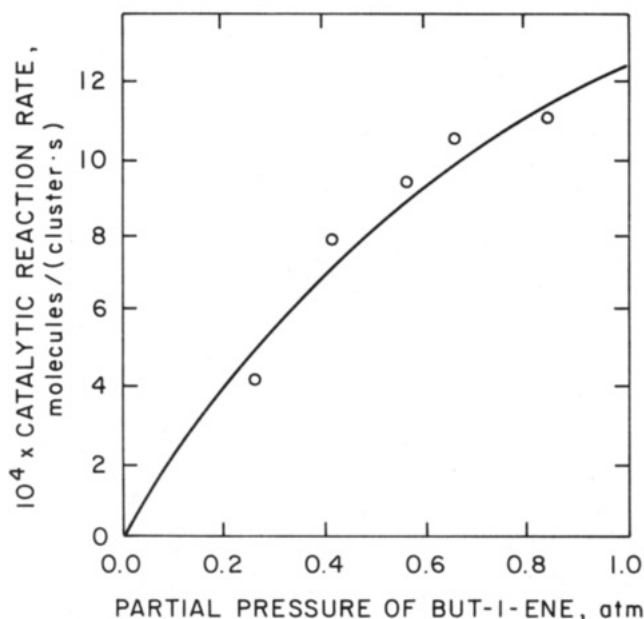


Figure 6. Kinetics of but-1-ene isomerization at 110 °C catalyzed by a polymer (sample 2). The curves represent the fit of eq 2 with the parameter values stated in the text.

TABLE III: Binding Energies (E_b) of Rh 3d_{5/2} and Os 4f_{7/2} Photoelectrons from XPS Results

sample	E_b /eV	
	Rh 3d _{5/2}	Os 4f _{7/2}
1. [H ₂ RhOs ₃ (acac)(CO) ₁₀ PPh ₂ -⊖] protected against air exposure	308.0	51.3
2. sample 1, air-exposed	308.0 sh, 309.0	51.4, 52.3 sh
3. sample 1, CO treated	308.0	51.3
4. sample 1, after use for butene isomerization	308.0	51.6
5. sample 1, after use for ethylene hydrogenation	308.2	51.3

the metal clusters or aggregates with diameters ≤ 1 nm were embedded within the polymer matrix; the membranes and clusters or aggregates contribute compatible intensities.⁹

Characterization of Catalysts by X-ray Photoelectron Spectroscopy (XPS). The fresh and used catalyst membranes were also characterized by XPS in an attempt to establish whether aggregated rhodium was present. The observed binding energies for the Rh 3d_{5/2} and Os 4f_{7/2} levels are summarized in Table III. These data show that the Rh 3d_{5/2} and Os 4f_{7/2} binding energies remained unchanged within the limits of accuracy during exposure of the sample to CO and during catalysis of but-1-ene isomerization or ethylene hydrogenation. Only the sample exposed to air showed a shift in binding energy: from 308.0 to 309.0 eV for Rh 3d_{5/2} and from 51.3 to 52.3 eV for Os 4f_{7/2}.

The Rh 3d_{5/2} binding energy of 308.0–308.2 eV (Table III) is significantly higher than that reported for metallic rhodium (307.1 eV).^{11a-d} Although less pronounced, the same trend was also observed for the Os 4f_{7/2} binding energy, which is reported to be 50.7 eV^{11b} for metallic osmium, in contrast to 51.3 eV for the anchored cluster [H₂RhOs₃(acac)(CO)₁₀PPh₂-⊖]. These higher binding energies than those of the metals are typical of carbonyl cluster compounds. A Rh 3d_{5/2} binding energy of 308.8

(9) An improvement of the signal-to-noise ratios could not be achieved with other embedding materials which would provide smaller specimen thickness, since the embedding resin does not penetrate into the membrane (as it does with biomolecules) and therefore contributes to the signal-to-noise ratio. Even smaller specimen thickness (the smallest thickness that can be achieved with an ultramicrotome is approximately 20–25 nm) would not improve the signal-to-noise ratio sufficiently to allow resolution of individual metal aggregates in the relevant size range by high-resolution electron microscopy.¹⁰

(10) Tesche, B.; Zeitler, E.; Delgado, E. A.; Knözinger, H. "Proceedings of the 40th Annual Meeting of the Electron Microscopy Society of America", Washington, DC, 1982, p 658.

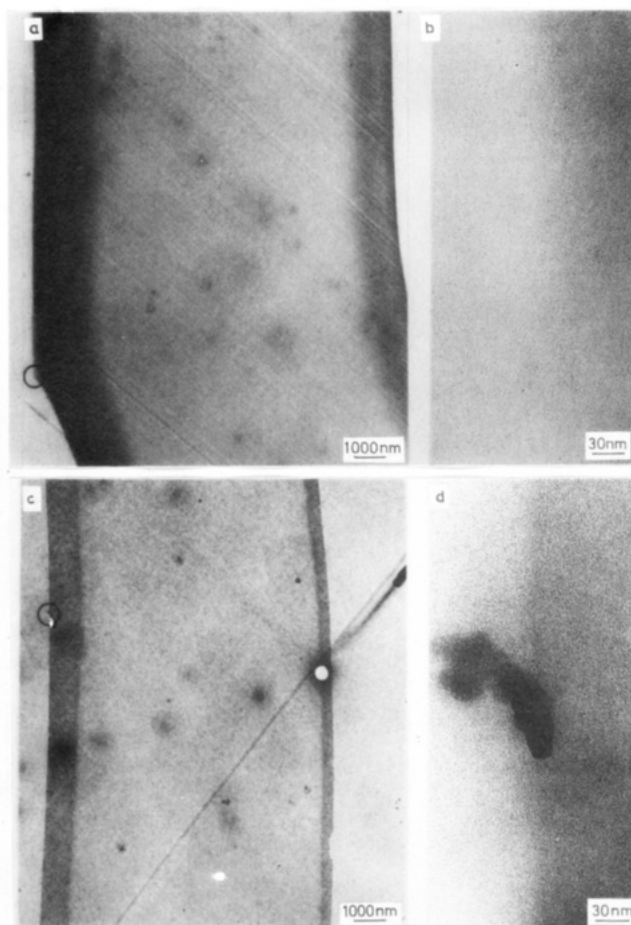


Figure 7. Electron micrographs of polymer-supported bimetallic catalysts after use in but-1-ene conversion (a and c) and ethylene hydrogenation (b and d). Micrographs a and c are cross-sectional views across the widths of the membranes; b and d show the circled areas from a and c, respectively, at higher magnification.

eV was reported^{11d} for [Rh₆(CO)₁₆], and an analogous trend was observed for platinum and platinum carbonyl clusters such as [Pt₃(CO)₆]_n.³⁻¹² The differences between the binding energies of metal atoms in a molecular cluster and in the bulk metal are explained by (a) withdrawal of electrons from the metal atoms by CO ligands and (b) reduced extraatomic relaxation relative to the bulk metal. The XPS results are thus in agreement with the infrared characterization, suggesting the presence of the intact RhOs₃ cluster in the fresh catalyst.

The Rh 3d_{5/2} and Os 4f_{7/2} binding energies remained essentially unchanged after exposure of the membrane to C₂H₄ + H₂ or to but-1-ene + H₂ mixtures at 100–130 °C for more than 15 h (Table III). We have inferred from the catalysis experiments that, as a result of the breakup of the original cluster, rhodium was aggregated into particles; the microscopy showed that there were no particles larger than 1 nm. The essentially unchanged intensity ratio of Rh/Os XPS peaks is consistent with the formation of highly dispersed metals, since significant rhodium aggregation would lead to a decrease of this ratio. Binding energies higher than those of the bulk metal have been reported previously for highly dispersed metal particles.¹³⁻¹⁵ We therefore infer that the Rh3d_{5/2} binding energy of 308–308.2 eV is characteristic of highly

(11) (a) Anderson, S. L. T.; Scurrill, M. S. *J. Catal.* **1979**, *59*, 340. (b) Fuggle, J. C.; Martensson, N. *J. Electron Spectrosc. Relat. Phenom.* **1980**, *21*, 275. (c) Andersson, S. L. T. *J. Catal.* **1981**, *71*, 233. (d) Andersson, S. L. T.; Watters, K. L.; Howe, R. F. *J. Catal.* **1981**, *69*, 212.

(12) Apai, G.; Lee, S.-T.; Mason, M. G.; Gerenser, L. J.; Gardner, S. A. *J. Am. Chem. Soc.* **1979**, *101*, 6880.

(13) Takasu, Y.; Unwin, R.; Tesche, B.; Bradshaw, A. M.; Grunze, M. *Surf. Sci.* **1978**, *77*, 219.

(14) Mason, M. G.; Baetzold, R. G. *J. Chem. Phys.* **1976**, *64*, 271.

(15) Huizinga, T.; van't Blik, H. F. J.; Vis, J. C.; Prins, R. *Surf. Sci.* **1983**, *135*, 580.

dispersed rhodium aggregates (size range <1 nm) formed within the membrane upon breakup of the original cluster.

After exposure of the sample to air, the Rh 3d_{5/2} and Os 4f_{7/2} binding energies were shifted to higher values (by approximately 1 eV, Table III), which suggests an oxidation of the metal species. The binding energy of 309 eV of Rh 3d_{5/2} electrons might indicate a Rh³⁺ oxidation state,¹⁶ and the shoulder at 52.3 eV of the Os 4f_{7/2} peak might be characteristic of Os²⁺ species.¹⁷

Conclusions

A unique cluster species was formed on the polymer support, as demonstrated by the infrared spectra, namely [H₂RhOs₃(CO)₁₀Ph₂P-⊖]. This is one of the few supported bimetallic species with a well-defined structure,¹⁸ and it therefore serves the purpose of this research, providing a defined starting material and allowing an opportunity to understand the changes in the structure as the catalyst evolves from the precursor through various stages of activity.

As expected, the coordinatively saturated [H₂RhOs₃(acac)(CO)₁₀Ph₂P-⊖] lacks catalytic activity for alkene isomerization and hydrogenation. The onset of catalytic activity after an induction period demonstrates that there were structural changes which led to the formation of coordinatively unsaturated species. The catalytic and infrared data indicate that the activity for alkene isomerization is associated with triosmium clusters and that for alkene hydrogenation with small aggregates of metallic Rh. The evidence provided by XPS and electron microscopy is consistent with this interpretation, but a direct demonstration of the Rh aggregates is still lacking. In summary, the results are consistent with the interpretation that the catalyst was formed by breakup of the initial bimetallic clusters, segregation of the metals, and aggregation of the Rh without significant breakup of the triosmium units.

Experimental Section

Catalyst Synthesis. Eleven-micrometer-thick membranes of a block copolymer poly(styrene-*co*-divinylbenzene-*co*-*p*-styryldiphenylphosphine) were prepared from the monomers according to a literature procedure.² The monomers styrene and divinylbenzene were vacuum distilled to remove the polymerization inhibitors present in the commercially available reagents.

[H₂RhOs₃(CO)₁₀(acac)] (I) and [H₂RhOs₃(CO)₁₀(acac)PPh₃] (II) were prepared by described procedures;⁷ all manipulations were done under an inert atmosphere. A polymer membrane (15 mg) incorporating 10% mol of -PPh₂ groups and a sufficient amount of I to give a -PPh₂/I molar ratio of 1/1.2 were placed in a flat-bottom flask equipped with a magnetic stirrer. The flask was cooled to -30 °C under N₂. THF (freshly distilled from Na/benzophenone under N₂) was cooled to -30 °C and slowly transferred into the reactor. The transfer was discontinued when the liquid volume (100 mL) was sufficient to cover the membrane. Rapid transfer of the THF (a good swelling agent for the mem-

brane) was avoided, since it may lead to rapid swelling and destruction of the membrane. The mixture was stirred at -20 °C for 10 min. The solution was removed and the membrane washed 3 times, each with 10 mL of THF, and dried under vacuum. The resulting orange membrane was stored under nitrogen. The samples were analyzed for P, Rh, and Os by Schwarzkopf Microanalytical Laboratory, Woodside, NY.

Catalytic Activity Measurements. The catalytic reactions were investigated with a flow reactor system allowing simultaneous measurement of reaction rates and infrared spectra of a functioning catalyst membrane. The reactant stream contained ethylene or but-1-ene fed from a high-pressure cylinder. The stream also usually contained H₂, He, and/or CO, which flowed from cylinders through an oxygen trap (incorporating particles of Cu catalyst activated in flowing H₂ at 200 °C for 2 h prior to each experiment) and a water trap (incorporating particles of zeolite 5A), activated in flowing He at 400 °C for 2 h prior to each experiment.

The reactants flowed through a cell held at constant temperature in the sample compartment of a Nicolet 7199 Fourier transform infrared spectrometer. The cell held a catalyst membrane perpendicular to the beam of the infrared radiation. Product gases flowed from the sample cell (the reactor) through a reference cell, and conversions were so low that the compositions of the gases in the two cells were nearly the same and their infrared absorptions nearly cancelled. Therefore, the observed spectra were indicative of the catalyst membrane in the working state.

Product gases flowing at steady state from the reference cell were periodically sampled and analyzed with an on-line gas chromatograph equipped with a flame ionization detector. The products of ethylene hydrogenation were separated in a 3 m × 3.2 mm stainless-steel column packed with Porasil C (80/100 mesh); the products of but-1-ene isomerization were separated in a column with Carbopack impregnated with 1.9 wt % picric acid.

Electron Microscopy of Catalysts. The membranes, exposed to air, were embedded in the resin ERL 4206.¹⁹ Thin sections (thickness ~50 nm) were cut on a Reichert Ultracut microtome with a diamond knife, mounted on Tornvas and carbon-coated grids (400 mesh). Electron micrographs were recorded with a Philips EM400T at varying magnifications.

X-ray Photoelectron Spectroscopy. The membranes were analyzed with a Physical Electronics AES/XPS system (Model 550), consisting of an ultrahigh-vacuum analysis chamber and a pretreatment chamber with high-vacuum facilities. The pressure in the analysis chamber during data acquisition was typically 5 × 10⁻⁹ torr.

XP spectra were obtained with a Mg radiation source and a cylindrical mirror analyzer. Signals were multiplexed and averaged to improve the signal-to-noise ratio. The acquisition time for each spectrum was 5 min, and checks were made to ensure that charging equilibrium had been reached and that spectral shifts were not indicative of equilibration of charging. The spectral resolution was 0.5 eV. Reported binding energies are referenced to the C 1s peak at 284.6 eV; they are accurate to ±0.2 eV.

Acknowledgment. This work was supported by grants from Air Products and Chemicals, Inc., the National Science Foundation, and the Deutsche Forschungsgemeinschaft.

Registry No. Rh, 7440-16-6; Os, 7440-04-2; H₂RhOs₃(acac)(CO)₁₀, 77674-51-2; H₂Os₃(CO)₁₀(PPh₃), 56398-26-6; H₂Os₃(CO)₉(PPh₃), 88510-52-5; poly(styrene-*co*-divinylbenzene-*co*-*p*-styryldiphenylphosphine), 39319-11-4.

(16) (a) Baranovskii, I. B.; Golubnidaya, M. A.; Ya Mazo, G.; Nefedov, V. I.; Salyu, Ya. V.; Shchelokov, R. N. *Russ. J. Inorg. Chem.* **1976**, *21*, 591. (b) Imanaka, T.; Kaneda, K.; Teranishi, T.; Terasawa, M. *Proc. Int. Congr. Catal.*, 6th **1976**, 509. (c) Contour, J. P.; Mouries, G.; Hoogewijs, M.; Leclerc, C. *J. Catal.* **1977**, *48*, 217.

(17) Knözinger, H.; Zhao, Y.; Tesche, B.; Barth, R.; Epstein, R.; Gates, B. C.; Scott, J. P. *Faraday Discuss. Chem. Soc.* **1981**, *72*, 53.

(18) Guzzi, L. In "Metal Clusters in Catalysis"; Gates, B. C., Guzzi, L., Knözinger, H., Eds.; Elsevier: Amsterdam, in press.

(19) Spurr, A. R. *J. Ultrastruct. Res.* **1969**, *26*, 31.